

Tensegrity Active Control: a Multi-Objective Approach

Bernard Adam¹ and Ian F. C. Smith, F.ASCE²

Abstract

A multi-objective search method is adapted for supporting structural control of an active tensegrity structure. Structural control is carried out by modifying the self-stress state of the structure in order to satisfy a serviceability objective and additional robustness objectives. Control commands are defined as sequences of contractions and elongations of active struts to modify the self-stress state of the structure. A two step multi-objective optimization method involving Pareto filtering with hierarchical selection is implemented to determine control commands. Experimental testing on a full-scale active tensegrity structure demonstrates validity of the method. In most cases, control commands are more robust when identified by multi-objective optimization method as compared with a single objective and this robustness leads to better control over successive loading events. Evaluation of multiple objectives provides a more global understanding of tensegrity structure behavior than any single objective. Finally, results reveal opportunities for self-adaptive structures that evolve in unknown environments.

CE Database subject headings: Structural control, Active control, Stochastic process, Struts, Cables

¹PhD Student, Structural Engineering Institute, EPFL-ENAC-IS-IMAC, EPFL, 1015 Lausanne, Switzerland. E-mail: bernard.adam@a3.epfl.ch

²Professor, Structural Engineering Institute, EPFL-ENAC-IS-IMAC, EPFL, 1015 Lausanne, Switzerland. E-mail: ian.smith@epfl.ch

Introduction

Tensegrities are spatial and lightweight structures composed of compressed struts and tensioned cables. Stability is assured by self-stress. Tensegrities are very flexible: small loads can induce large displacements. We thus focus on serviceability control in order to provide new opportunities for large structures. Control is carried out by modifying the self-stress state of the structure through contracting or elongating active struts of a full-scale active tensegrity structure built at EPFL (Figure 1). Vertical displacements of three nodes of the top surface edge are measured with displacement sensors.

Previous studies have revealed that many combinations of contractions and elongations of active members can satisfy the serviceability objective of maintaining top surface slope when the structure is subjected to a loading situation (Fest et al. 2004), (Domer and Smith 2005). Therefore, this control task could be improved by employing multiple objectives to select the best control set. In structural engineering, researchers have focused mainly on applying multi-objective optimization methods to design tasks (Aguilar Madeira et al. 2005; Maute and Rauli 2004; Park and Koh 2004; Fonseca and Fleming 1998a 1998b; Kramer and Grierson 1989). Solving a design task involves building a set of good solutions that can be discussed by experts. We propose that a structural control task can be viewed as a multi-design task for multiple loading situations. However, since no expert discussion is possible, automatic single solution selection is needed. This second type of task can be classified as a dynamic multi-objective problem: objective functions, constraints and associated parameters may be time dependent (Farina et al. 2004).

One of the few examples of a multi-objective optimization method used for control was presented by Hau and Fung (2004). The scope of this numerical study involved controlling

the shape of a flexible multi-layer beam using a multi-objective genetic algorithm. Objectives are maintaining structural shape and minimizing input voltage for the active system. In the broader civil engineering domain, two control tasks have been supported with a multi-objective optimization method. They are both related to water supply (Baràn et al. 2005; Chuntian and Chau 2002). These studies are numerical; no experimental testing was performed. Other control tasks that are supported using multi-objective optimization are far from structural engineering: shop floor scheduling (Hong and Prabhu 2004), multi-objective control for a robotic manipulator (Win and Cheah 2004), a power dispatch task (Zhang and Zhen, 2004), portfolio control and optimization (Derigs and Nichel 2004) and ecology (Brouwer and Van Ek 2004).

Even for one objective, few studies focus on tensegrity control. Averseng and Crosnier (2004) studied the control of a tensegrity grid where actuation system is connected to the supports. Other studies of tensegrity control have been conducted mainly through numerical simulation. Kanchanasaratool and Williamson (2002) proposed a dynamic model to study tensegrity feedback shape control. Skelton et al. (2000) concluded that since only small amounts of energy are needed to change the shape of tensegrity structures, they are advantageous for active control. Sultan (1999) proposed a formulation of tensegrity active control and illustrated it with the example of an aircraft motion simulator. Djouadi et al. (1998) described a scheme to control vibrations of tensegrity systems.

Our research involves development of computational control, numeric simulation and experimental testing. This paper describes how control commands are determined through multi-objective optimization. Experimental validation is then carried out on a full scale active tensegrity structure.

Previous work

Research into active structures has been carried out at EPFL since 1996. Fest (2002) designed and built the laboratory structure and the control system. The topology was proposed by Passera & Pedretti, Lugano (Switzerland) in order to limit the buckling length of compressed members. It contains 5 modules and covers a surface area of 15m^2 for a static height of 1.20m and a mass of 30kg/m^2 . It is composed of 30 struts and 120 tendons. Struts are fiber reinforced polymer tubes of 60mm diameter and 703 mm^2 cross section. Tendons are stainless steel cables of 6 mm in diameter.

The structure rests on three supports that allow statically determinate support conditions. Struts converge toward a central node where connection is provided by contact compression on a steel ball. In this node, compressive forces always converge to the center of the steel ball. It thus avoids eccentricities that can lead to instability while controlling the structure. The structure is equipped with 10 actuators (active members). They are placed in pairs in-line within each of the five modules and make it possible to change length of active struts (Figure 2). Vertical displacements of three nodes of the top surface edge of the structure are measured with inductive displacement sensors.

The objective of the study was to determine control commands (sequence of contractions and elongations of active struts) that are able to satisfy a serviceability objective: maintaining the slope of the top surface of the structure constant when subjected to a load. Slope is determined through vertical displacement measurements at three nodes: 37, 43 and 48 (Figure 3). This objective is a control criterion that could be useful for structures such as antennas, pedestrian bridges and temporary roofs. A single objective stochastic search algorithm (PGSL: Probabilistic Global Search Lausanne) was selected as the best stochastic search

method to accommodate the combinatorial generate-test process that identifies control commands (Domer et al 2003). PGSL is a direct search algorithm developed at EPFL (Raphael and Smith, 2003).

Although structural calculations that determine structural position using preset strut lengths and loading as input is straightforward with the dynamic relaxation method, the inverse operation of determining strut-length changes to achieve a required behaviour of the structure is much more difficult. Closed form methods are unsuccessful because of geometrical non-linearities, high coupling between elements, coupling between the effect of actuators and the presence of local minima in the solution space. Once validated, control commands that are found by stochastic search are then applied to the laboratory structure. This study concludes that a stochastic search algorithm and dynamic relaxation have much potential for satisfying a serviceability objective for an active tensegrity structure.

Domer and Smith (2005) studied the capacity of the structure and its control system to learn. A generate-test process was used with stochastic search and case-based reasoning. In order to take advantage of previous experience, altered configurations and corresponding control commands are stored in a case-base. When the structure is subjected to a load, the nearby configuration is retrieved from the case base and its control command is adapted to the new task. As cases are added to the case-base the average time necessary to identify and adapt a control command decreases (learning). Domer (2003) showed that search time can decrease from approximately one hour down to a few minutes. Since the structure is able to improve performance progressively using past experience, we consider this to be an aspect of intelligence. Clustering cases in the case-base was also proposed to speed up the retrieval process. Maintenance of the case-base is crucial to prevent consuming too much time for

retrieval. In addition, an artificial neural network was used to model inaccuracies due to joint friction which are not taken into account in the computational model (Domer and Smith 2005). Trough correcting the numerical model with neural network accuracy of predictions was enhanced. This study concludes that structural performance could be enhanced by judicious combinations of advanced algorithms. However control commands were identified using a single objective (slope). This approach cannot therefore ensure robustness of the structure and the active control system for subsequent loading and control commands. A multi-objective methodology is reviewed in the following section.

Methodology

Previous studies have revealed that many combinations of contractions and elongations of active struts can satisfy a single serviceability objective to an acceptable degree. This presents an opportunity to enhance control command search through use of additional objectives. Additional objectives should not significantly decrease control command quality with respect to the slope objective. Goals are to increase robustness of both the structure and the active control system in order to carry out multiple control events over service lives. The following four conflicting objectives are used to guide search:

- Slope: maintain top surface slope of the structure constant when subjected to loading,
- Stroke: maintain actuator jacks as close as possible to their midpoint,
- Stress: minimize stress of the most stressed element,
- Stiffness: maximize the stiffness of the structure.

The general form of a multi-objective optimization problem can be expressed as follows:

$$\begin{array}{ll} \text{Minimize objective functions} & f(\mathbf{x}) \\ \text{subject to inequality constraints} & \mathbf{g}(\mathbf{x}) \leq 0 \end{array}$$

and equality constraints $\mathbf{h}(\mathbf{x}) = 0$

where $\mathbf{x} \in \mathbb{R}^n$, $\mathbf{f}(\mathbf{x}) \in \mathbb{R}^k$, $\mathbf{g}(\mathbf{x}) \in \mathbb{R}^m$, and $\mathbf{h}(\mathbf{x}) \in \mathbb{R}^p$. Here, n represents the number of variables, k the number of objective functions, m the number of inequality constraints and p the number of equality constraints.

Decision variables, objective functions and constraints of the active tensegrity structure multi-objective control task are expressed as follows in the above notation:

Decision variables are the position of the ten actuators:

$$\mathbf{x} = (x_1, x_2 \cdots x_{10})$$

The 4 objective functions (slope, stroke, stress and stiffness) are expressed mathematically below. Distance between current slope and initial slope is minimized:

$$f_{slope} = [S(\mathbf{x}, \mathbf{q}) - S^0]^2$$

where S is the slope of the top surface of the structure, \mathbf{q} is the load case set and S^0 is the initial slope of the top surface. Slope is formally expressed as follows:

$$S = \left(z_{43} - \frac{z_{37} + z_{48}}{2} \right) / L$$

where z_i is the vertical coordinate of node i and L the horizontal length between node 43 and the middle of segment 37 – 48 (Figure 3). Slope unit is mm/100m. The aggregate distance between actuator position and mid point has also to be minimized:

$$f_{stroke} = \sum_{i=1}^{10} (x_i - x_i^0)^2$$

where x_i^0 is the midpoint position of the i th actuator.

The stress in the element that is the closest to its limit is minimized:

$$f_{stress} = \max \left(\frac{N(\mathbf{x}, \mathbf{q})_{strut, \max}}{N_{strut, \lim}}, \frac{N(\mathbf{x}, \mathbf{q})_{cable, \max}}{N_{cable, \lim}} \right)$$

where $N_{strut,max}$ is the maximum compression force in the struts, $N_{cable,max}$ is the maximum tension force in the cables, $N_{strut,lim} = -20 \text{ kN}$ is the limit compression force in struts which corresponds to the half of the buckling load limit and $N_{strut,lim} = 8.5 \text{ kN}$ is the limit tension force in cables which corresponds to the half of the rupture limit.

Maximizing stiffness is equivalent to minimizing compliance indicator:

$$f_{stiffness} = \frac{1}{K}$$

For the purposes of this study, an approximate global stiffness indicator is expressed as follows:

$$K = \frac{Q_{37} + Q_{43} + Q_{48}}{|\Delta S(Q_{37})| + |\Delta S(Q_{43})| + |\Delta S(Q_{48})|}$$

where $\Delta S(Q_i)$ is the slope variation induces by the vertical downward point load $Q_i = 1000 \text{ N}$, at node i . Since Q_i is expressed in N and $\Delta S(Q_i)$ in $\text{mm}/100\text{m}$, the units of this indicator are $N/(\text{mm}/100\text{m})$.

Inequality constraints are intended to prevent failure at the compensated slope. Strut buckling and cable rupture have to be avoided. Since stability of the structure is provided by self stress between struts and tendons, and since strut connections are made through contact compression only, tension in struts has to be avoided. Constraints also bound actuator positions. No equality constraints are used for this task. Constraint functions have the following expressions:

$$g_{no_buckling} = -(N(\mathbf{x}, \mathbf{q})_{strut,max} - N_{strut,lim}) \leq 0$$

$$g_{no_tension} = N(\mathbf{x}, \mathbf{q})_{strut,min} \leq 0$$

$$g_{no_rupture} = N(\mathbf{x}, \mathbf{q})_{cable,max} - N_{cable,lim} \leq 0$$

$$g_{x,min} = -(x_i - x_i^{\min}) \leq 0, \quad \forall i = 1, \dots, 10$$

$$g_{x,\max} = x_i - x_i^{\max} \leq 0, \forall i = 1, \dots, 10$$

A Pareto filtering approach is employed in order to avoid the use of weight factors. In case of a multi-objective minimization task, a solution x^* is said to be Pareto optimal if there exists no feasible vector of decision variables x which would decrease some objective without causing a simultaneous increase in at least one other objective. This concept results in a set of solutions called the Pareto optimal set. The vectors x^* corresponding to the solutions included in the Pareto optimal set are called non-dominated (Pareto, 1896).

The multi-objective search method adapted to our tensegrity structure serviceability control task involves building a Pareto optimal solution set and selecting one solution (Figure 4). The Pareto optimal solution set is identified according to the four objectives and the five constraints described above. Solution generation and Pareto filtering are carried out using the ParetoPGSL algorithm. Solutions are generated in order to minimize all objectives. Dominated solutions are rejected. Dominated solutions are defined as solutions that are as good as a Pareto optimal solution with respect to all objective but at least one. ParetoPGSL stops after 1500 generated solutions since preliminary studies showed that solution quality does not improve further.

The selection strategy that is adopted hierarchically reduces the solution space until identification of a control command. It is developed in four steps and reflects the importance of the objectives. Control commands for which slope compensation is less than 95% are first rejected. In practical situations, slope compensation would be acceptable if its value was above this threshold. To keep objectivity with respect to the three remaining objectives, the remaining solutions are divided into thirds according to solution quality. The worst third of the solutions with respect to the stroke objective is rejected. The worst half of the remaining

solutions with respect to the stress objective is then rejected. Finally, the best solution with respect to the stiffness objective is identified among solutions that are left. This becomes the control command that is applied to the structure. Therefore, each of the three objectives in the last three steps leads to rejection of the same number of solutions.

Control solutions describe the structural configuration when slopes are compensated. Sequences of application of control commands that transform the altered slope state to the compensated slope state involve verifying that no failure would happen during intermediate steps. The control command is divided into 1 mm steps. Strut contractions are placed at the beginning of the sequence and strut elongations at the end. In this way, energy is generally first taken out of the structure before it is added. Calculations are made using the dynamic relaxation method. The position of the structure is evaluated for each 0.1 mm of actuator travel. The sequence is then applied to the laboratory structure for experimental validation.

Results

This methodology is tested for 24 load cases involving up to two vertical downward point loads from 391 N to 1209 N in magnitude (Table 1). A view of the structure from above is showed in Figure 3. Examine load case 5: 859 N point load at node 32. Pareto optimal solutions are generated using the ParetoPGSL algorithm (Figure 5). Solutions are presented in four dimensions with respect to the four objectives. The slope objective is shown on the vertical axis. Stroke and stress objectives are represented with the horizontal axis. The gray bar evaluates the stiffness objective. Values close to zero are considered best for all objectives.

The first step of the hierarchical selection strategy consists of rejecting all solutions for which slope compensation is less than 95% (Figure 6).

The second step of the selection strategy involves dividing the remaining solution set into three parts according to stroke objective. The worst third is rejected (Figure 7).

The third step of the selection strategy results in dividing the remaining solution set into two parts according to stress objective quality. The worst half is rejected (Figure 8).

The last step of the selection strategy consists of identifying the control command as the best solution with respect to stiffness objective. (Figure 8). This solution is the control command that is used to control the structure.

The application sequence of this control command is then calculated to verify that no failure would happen and to observe slope evolution. The control command is applied to the loaded laboratory structure for experimental validation (Figure 9). Slope deviation evolution is plotted against steps of 1mm of actuator travel. As said previously, for the purpose of this study, slope unit is *mm/100m*. Slope deviation is the difference between initial slope and current slope. It is equal to zero when initial slope is recovered. Slope compensation is defined to be:

$$SC = \frac{CS - AS}{IS - AS}$$

Where *CS* is the corrected slope when the control command has been applied, *AS* the altered slope and *IS* the initial slope. Numerical simulation gives an altered slope deviation of -147mm/100m and a corrected slope deviation of 1mm/100m (99% compensated). Experimental testing gives an altered slope deviation of -138mm/100m and a corrected slope deviation of -4mm/100m (97% compensated). The average actuator travel is 1.5 mm. The most tensioned cable at the compensated slope state is cable 15 with 7.8 kN (92% of limit tensile force) whereas the most compressed strut is strut 145 with 17.8 kN (89% of limit

compression force). Stress values are only numerical because the structure is not equipped with force sensors that would provide experimental data. Simulation and laboratory test results for slope are generally in good agreement.

Control command robustness improvement is shown in Figures 10 – 13 for the 24 load cases listed in Table 1. Comparison of slope compensation between single objective (slope) and multi-objective search for one and two point loads is presented in Figure 10. Slope compensation quality does not decrease significantly with multi-objective optimization when stroke, stress and stiffness are also taken into account. Figure 11 shows the average stroke for commands identified using a single objective and multi-objective methods. In 17 cases out of 24, average stroke is less when the control command is identified with multi-objective search. Since multi-objective methods are intended to satisfy multiple objectives, solutions are trade off solutions. Nevertheless, multi-objective solutions are more robust than single objective solutions. Figure 12 shows the comparison of the limit load ratio of the most stressed element when slope is compensated, for control command identified using single objective (slope) and multi-objective search. In the 24 cases, the limit load ratio is less when slope is compensated with multi-objective control command. Figure 13 shows stiffness comparison when slope is compensated with control commands identified using single objective (slope) and multi-objective search. Since the stiffness objective is the last objective to be employed it is more difficult to improve stiffness using multi-objective search. Conflicts between objectives are also illustrated in Figure 10 – 13. In 5 cases out of 24, control command quality with respect to all three robustness objectives is improved when the control command is identified with multi-objective search. In 18 cases, control command quality is improved for two robustness objectives. Load case 3 exhibits quality improvement only for the stress objective.

More experimental validation is presented in Figures 14. Slope compensation correlation between numeric simulation and experimental testing is plotted in this diagram. Very good agreement between experimental testing and numeric simulation can be seen when the point load is placed at nodes 26, 32, 48, 41, 50 or 45, with a correlation between 80% and 100%. Correlation is between 60% and 80% for the other load cases. Deviation between numeric simulation and experimental testing increases when altered slope increases. This is probably due to friction in the connections and to the non-linear effect of the control command application.

These results are obtained from altered slope compensation due to a single loading event. We now introduce the concept of multi-objective serviceability control when the structure is subjected to a scenario of sequentially applied loads. This scenario simulates multiple control events over service life. To illustrate this situation, consider the multiple load applications presented in Table 2. Structural control for this scenario is presented in Figure 15. Slope evolution is plotted versus steps of 1mm of actuator travel. Load events are numbered from 1 to 6. Zero slope deviation means that initial slope is recovered. Structural behavior when control commands are identified using multi-objective search and single objective search are evaluated. Control commands are more rapidly effective when they are identified with multi-objective search. Single objective control command exhibit a more pronounced zig-zag profile that requires more steps to correct the slope. Multi-objective commands are useful to maintain robustness of both the structure and the control system whereas in single objective sequence no such maintenance can be assured. At the sixth control command, the multi-objective method makes it possible to compensate the slope whereas a single objective method leads to buckling of a strut.

Conclusions

Control commands are defined according to the load case and four objectives: top surface slope compensation, stroke, stresses and stiffness. The following conclusions come out of this research:

- Control commands are, in most cases, more robust when determined by multi-objective control as compared with single objective (slope) control.
- In situations where satisfying a dominant objective results in many solutions, a Pareto approach together with hierarchical elimination of solutions is attractive, especially when tasks require single solutions such as during structural control.
- Evaluation of multiple objectives provides a more global understanding of tensegrity structure behavior than any single objective.
- Multiple load application events are controlled more efficiently using multi-objective control.

These results lead toward more autonomous and self-adaptive structures that evolve in changing environments.

Acknowledgments

The authors would like to thank the Swiss National Foundation for supporting this work. Dr. E. Fest built the structure and the control system. Dr. B. Domer improved control and implemented the case-based reasoning study. Prof. B. Raphael provided support during programming of the control system. We are also grateful to Dr. K. Shea (University of Cambridge, UK), Passera & Pedretti SA (Lugano, Switzerland) and P. Gallay (EPFL, Switzerland) for their contributions.

Notation

The following symbols are used in this paper:

f	=	Vector of objective functions
g	=	Vector of inequality constraints
h	=	Vector of equality constraints
K	=	Structure global stiffness
N	=	Normal force
Q	=	Point load
q	=	load case set
S	=	Top surface slope
x	=	Decision variables set

References

- Aguilar Madeira, J.F., Rodrigez, H., and Pina, H., (2005), "Multi-objective optimisation of structures topology by genetic algorithms", *Advances in Engineering Software*, 36, 21-28.
- Averseng, J., and Crosnier, B., (2004), "Static and Dynamic Robust Control of Tensegrity Systems", *Journal of The International Association for Shell and Spatial Structures*, 45, 169-174.
- Baran, B., von Lücken, C., and Sotelo, A., (2005), "Multi-objective pump scheduling optimisation using evolutionary strategies", *Advances in Engineering Software*, 36, 39-47.
- Brouwer, R., and van Ek, R., (2004), "Integrated ecological, economic and social impact assessment of alternative flood control policies in the Netherlands", *Ecological Economics*, 50, 1-21.
- Chuntian, C., and Chau, K.W., (2002), "Three person multi-objective conflict decision in reservoir flood control", *European Journal of Operational Research*, 145, 625-631.
- Derigs, U., and Nickel, N.-H., (2004), "On a local-search heuristic for class of tracking error minimization problems in portfolio management", *Annals of Operational Research*, 131, 45-77.
- Djouadi, S., Motro, R., Pons, J.C., and Crosnier, B., (1998), "Active Control of Tensegrity Systems", *Journal of Aerospace Engineering*, 11, 37-44.
- Domer, B., and Smith, I.F.C., (2005) "An Active Structure that learns", *Journal of Computing in Civil Engineering*, 19(1), 16-24.
- Domer, B., Raphael, B., Shea, K. and Smith, I.F.C. (2003), "A study of two stochastic search methods for structural control", *Journal of Computing in Civil Engineering*, 17(3), 132-141.

- Domer, B., (2003). "Performance enhancement of active structures during service lives",
Thèse no 2750, Ecole Polytechnique Fédérale de Lausanne.
- Farina, M., Deb, K., and Amato, P., (2004), "Dynamic multi-objective optimization problems: test cases, approximations, and applications", IEEE Transactions on evolutionary computation, 8(5), 425-442.
- Fest, E., Shea, K., and Smith, I.F.C., (2004), "Active Tensegrity Structure", Journal of Structural Engineering, 130(10), 1454-1465.
- Fest, E., (2002). "Une structure active de type tenségrité", Thèse no 2701, Ecole Polytechnique Fédérale de Lausanne.
- Fonseca, C.M., and Fleming, P.J., (1998a), "Multiobjective Optimization and Multiple Constraint Handling with Evolutionary Algorithms-Part I: A Unified Formulation", IEEE Transactions on systems, man and cybernetics-Part A: Systems and humans, 28(1), 26-37.
- Fonseca, C.M., and Fleming, P.J., (1998b), "Multiobjective Optimization and Multiple Constraint Handling with Evolutionary Algorithms-Part II: Application Example", IEEE Transactions on systems, man and cybernetics-Part A: Systems and humans, 28(1), 38-47.
- Hau, L.C., and Fung, E.H.K., (2004), "Multi-objective optimization of an active constrained layer damping treatment for shape control of flexible beams", Smart Material and Structures, 13, 896-906.
- Hong, J., and Prabhu, V.V., (2004), "Distributed Reinforcement Learning Control for Batch Sequencing and Sizing in Just-In-Time Manufacturing Systems", Applied Intelligence, 20, 71-87.
- Kanchanasaratool, N., and Williamson, D., (2002), "Modelling and control of class NSP tensegrity structures", International Journal of Control, 75(2), 123-139.

- Kramer, G.J.E., and Grierson, D.E., (1989), "Computer automated design of structures under dynamic loads", *Computers & Structures*, 32(2), 313-325.
- Maute, K., and Rauli, M., (2004), "An interactive method for the selection of design criteria and the formulation of optimization problems in computer aided optimal design", *Comp. and Struct.*, 82, 71-79.
- Pareto, V., (1896), "Cours d'Economie Politique", vols I and II, Rouge: Lausanne, Switzerland.
- Park, K.-S., and Koh, H.-M., (2004), "Preference-based optimum design of an integrated control system using genetic algorithms", *Advances in Engineering Software*, 35, 85-94.
- Raphael, B. and Smith, I.F.C., (2003) "A direct stochastic algorithm for global search", *J of Applied Mathematics and Computation*, 146(2-3), 729-758.
- Skelton, R.E., Helton, J.W., Adhikari, R., Pinaud, J.P. and Chan, W., (2000), "An introduction to the mechanics of tensegrity structures", *Handbook on mechanical systems design*, CRC, Boca Raton, Fla.
- Sultan, C., (1999) "Modeling, design and control of tensegrity structures with applications", PhD thesis, Purdue Univ., West Lafayette, Ind.
- Win, K.K.K., and Cheah, C.-C., (2004), "Multi-objective learning control for robotic manipulator", *Journal of Robotic Systems*, 21(10), 539-557.
- Zhang, Y.-j., and Zhen, R., (2004), "Real-time optimal reactive power dispatch using multi-agent technique", *Electric Power Systems Research*, 69, 259-265.

Tables

Table 1. Downward load cases applied to the structure

Load case	Node	Magnitude [N]
1	26	-625
2	26	-900
3	26	-1209
4	32	-625
5	32	-859
6	32	-1092
7	37	-391
8	37	-550
9	37	-700
10	48	-391
11	48	-550
12	48	-700
13	6	-1092
14	37 and 45	-391
15	37 and 45	-624
16	37 and 45	-742
17	39 and 48	-157
18	39 and 48	-215
19	39 and 48	-274
20	41 and 50	-391
21	41 and 50	-624
22	45 and 48	-391
23	45 and 48	-624
24	45 and 48	-742

Table 2. Successive load event scenario

Load event	Node	Magnitude [N]
1	32	-391
2	50	-391
3	37	-391
4	48	-391
5	26	-391
6	6	-150

Figures

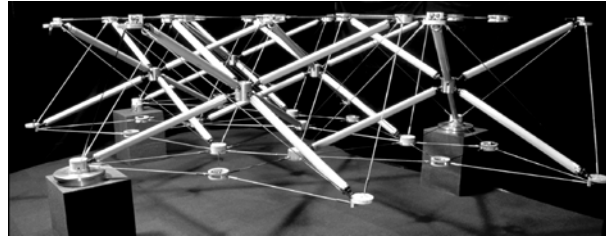


Fig. 1. Five module, 15m² ground projection area of the tensegrity structure built at EPFL

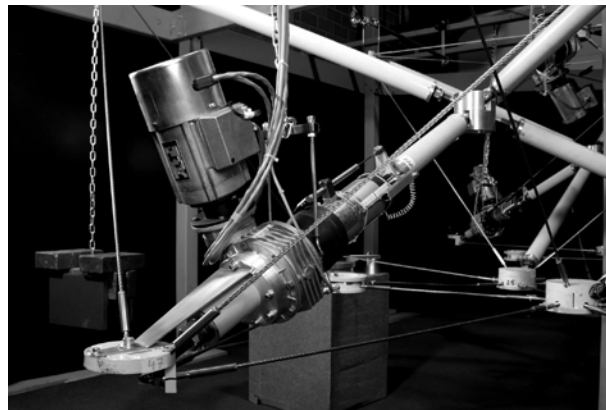


Fig. 2. Actuator: modify self-stress state by changing length of active members

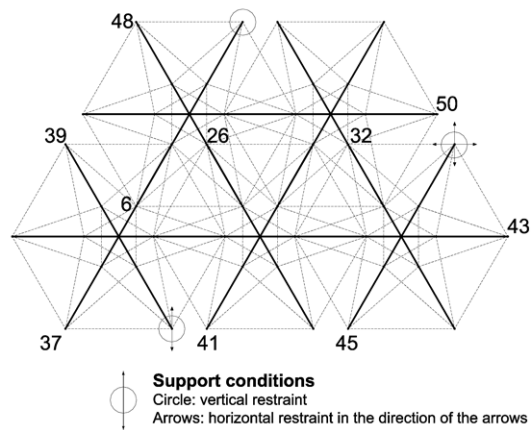


Fig. 3. View of the structure from above, with loaded nodes and support conditions

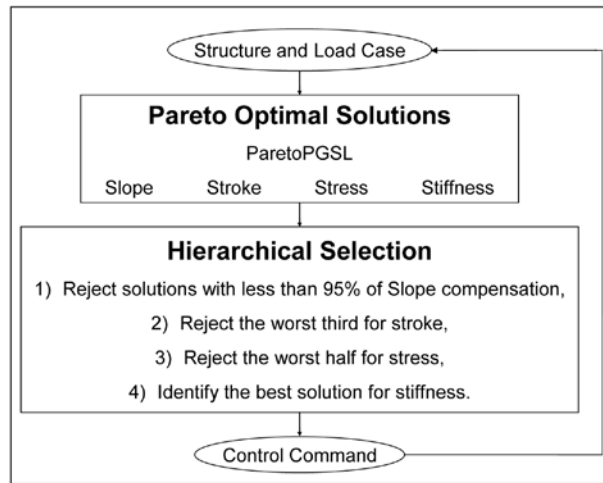


Fig. 4. Multi-objective methodology: Pareto optimal solutions and hierarchical selection

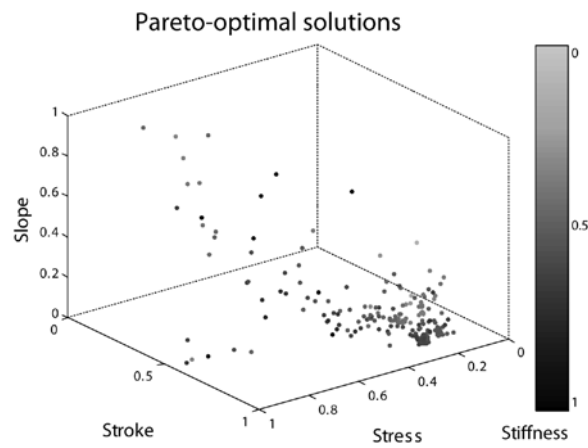


Fig. 5. Pareto optimal solutions with respect to slope, stroke, stress and stiffness objectives

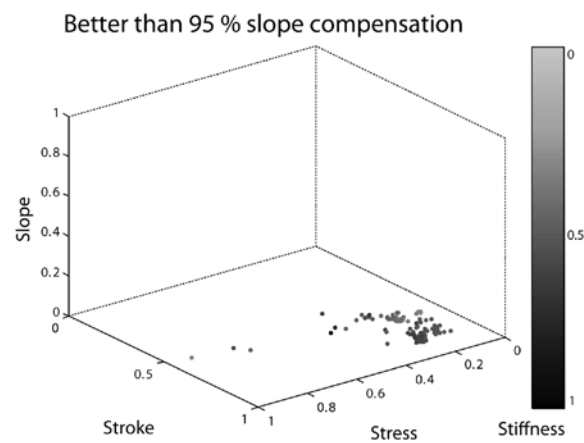


Fig. 6. Solutions for which slope compensation is better than 95%

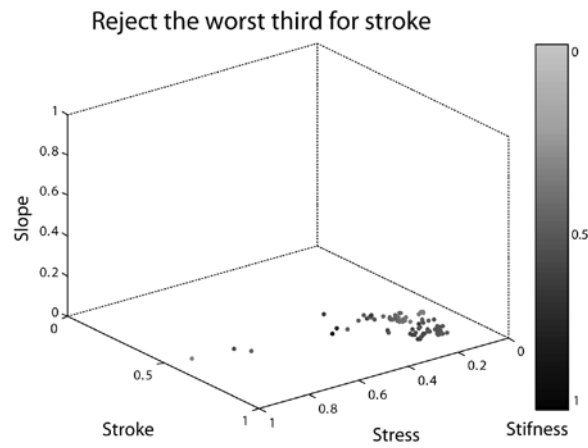


Fig. 7. Solutions for which the worst third of the previous set with respect to stroke has been rejected

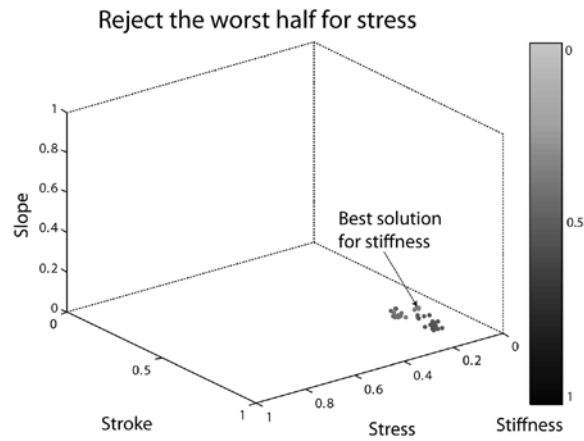


Fig. 8. Solutions for which the worst half of the previous set with respect to stress has been rejected

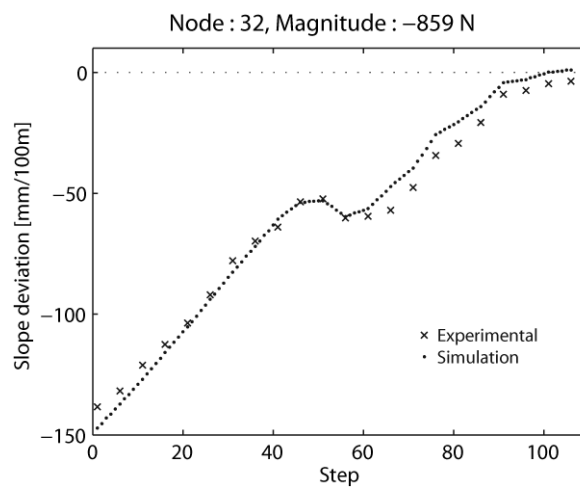


Fig. 9. Experimental and numerical slope compensation sequence

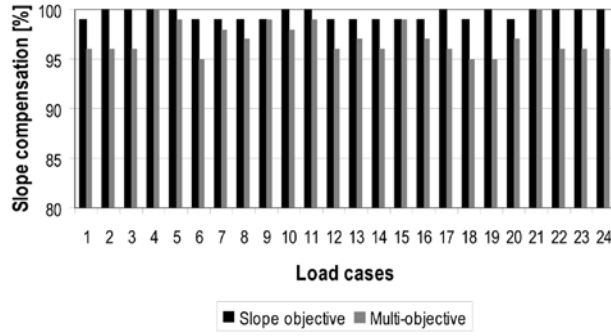


Fig. 10. Slope compensation for one (load cases 1-13) and two (load cases 14-24) point load

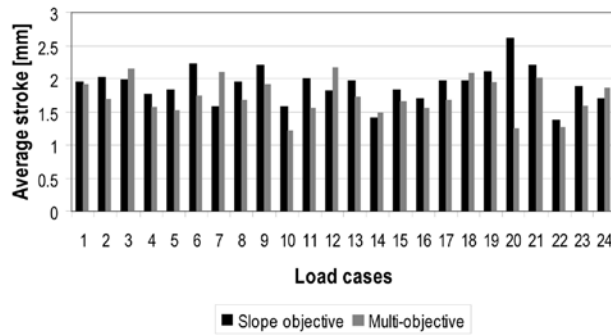


Fig. 11. Average stroke comparison for single objective or multi-objective search, for one (load cases 1-13) and two (load cases 14-24) point load

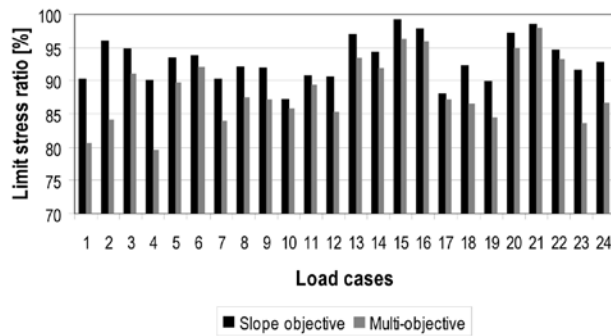


Fig. 12. Limit stress ratio for single objective and multi-objective search, for one (load cases 1-13) and two (load cases 14-24) point load

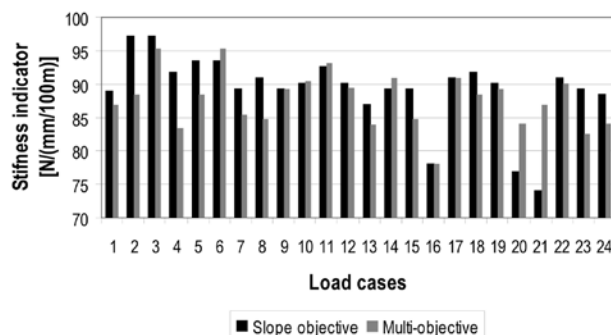


Fig. 13. Stiffness when slope is compensated, for single objective and multi-objective search, for one (load cases 1-13) and two (load cases 14-24) point load

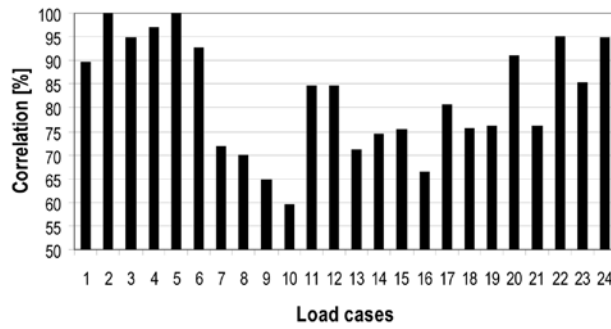


Fig. 14. Slope compensation correlation between numerical simulation and experimental testing, for one (load cases 1-13) and two (load cases 14-24) point load

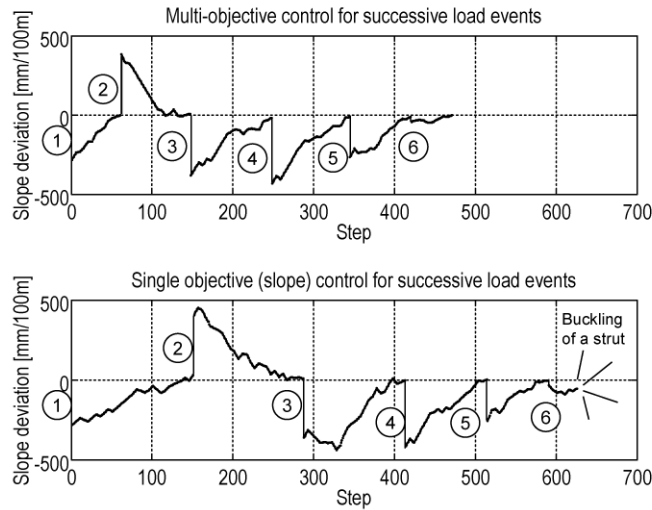


Fig. 15. Successive load events numbered from 1 to 6: multi-objective and slope-objective control commands behavior